INFLUENCE OF ROUGHNESS ON THE TRIBOLOGICAL BEHAVIOR OF A STEEL-STEEL COUPLE LUBRICATED WITH THREAD COMPOUND

N.A. ZABALA†, P.A. CASTRO‡ and W.R. TUCKART†,

† *Tribology Group, Engineering Department, Universidad Nacional del Sur - CONICET Av. Alem 1253, 8000 - Bahía Blanca, Bs. As. – Argentina wtuckart@uns.edu.ar;*
‡ *Surface Chemistry & Coatings Department, TenarisSiderca R&D Center (REDE-AR), Simini 250, 2804 - Campana, Bs. As. – Argentina. pcastro@tenaris.com*

***Abstract*— The purpose of this study is to determinate the influence of surface roughness on the tribological behavior of a lubricated steel against steel tribosystem. Tests were carried out at high pressure and slow sliding speed, in order to simulate at small scale, the contact conditions found in the seal of the threaded joints used in oil & gas casing and tubing strings.**

Tests were carried out with a simplified block-on-ring test, varying the surface roughness of rings between 1.3 to 3 μm R_a values. A thread compound lubricant containing lead, copper, zinc and graphite was used. During each cycle of test, the normal load was varied linearly between 250 N and 7000 N.

An exponential correlation between R_a and R_t roughness values with the wear damage was found and the wear damage of the blocks decreases about 40 percent with the increasing of initial Ra roughness parameter in the movil surface.

***Keywords*— Thread Compound; Surface Roughness; Friction; Greases.**

I. INTRODUCTION

Connection failures in oil and gas casing and tubing strings can lead not only to costly production delays and repairs but also to potential safety and environmental hazards. Thus, there is high interest in improving the tribological performance and reliability of fittings used in tubes in production wells.

During the make-up and break-out of the connections (Make & Break operations), threaded joints are subjected to intense mechanical and tribological solicitations. The performance of an Oil Country Tubular Good (OCTG) connection is not only dependent upon its geometry and material properties, but is also influenced, among others, by surface roughness and topography as well as surface treatments and thread compound (Bollfrass, 1983; Matsuki *et al.*, 1985).

Several thread compounds are used in the oil and gas industry. The most widely used lubricants, based on API RP 5A3 standard, contain heavy metals such as lead, copper and zinc. The solid additive used in largest amount is lead powder, which provides excellent anti-galling properties. Lead is rolled or compacted between the contact surfaces, preventing the metal-metal contact (Carper *et al.*, 1995; Carper *et al.*, 1992; Ertas *et al.*, 1999).

Two of the most important surface properties are roughness and topography. In order to improve the design of contact surfaces, it is important to understand the influence of surface roughness on friction and wear. The R_a parameter is the arithmetic mean of the profile deviation of the filtered roughness profile, and the R_t parameter is the vertical distance between the highest peak and the deepest valley within the measuring length. From the technological point of view, the average surface roughness (R_a) and the total roughness depth (R_t) are the most used parameters for surface roughness description.

Sedlaček *et al*. (2009) evaluated the influence of surface preparation on roughness parameters, friction and wear using a pin-on-disc test with dry and lubricated conditions. They concluded that abrasion was the dominant wear mechanism for dry tests and so the coefficient of friction (COF) was lower when roughness was higher. However, for lubricated tests, the opposite trend was found, which was explained by a better EHD (elastohydrodynamic) lubrication.

Muster and Presz (1999) study the influence of the Ra parameter on the galling behavior under dry cold metal-forming test. They determinated that the rough surface samples, R_a = 0,67 μm, are more inclined to avoid galling damage than surfaces with lower R_a parameter values.

Although a lot of work has been done, according to the recommended practice API RP 5A3 / ISO 13678: 2000, there is not yet a standard laboratory scale test to accurately reproduce the behavior of threaded joints. Furthermore, in the open literature there are only a few publications on the influence of the roughness on the tribological behavior for these applications.

In this sence, using a pin-on-box rotating test Carper *et al.* (1992) studied the effect of L80 and J55 steels with different manufacturing and operating variables on the COF in OCTG connections. They showed little differences in the COF value by changing the surface roughness of R_a between 0.37 μm and 1.5 μm. Moreover, in addition to studying different contact geometries and lubricants, Carper *et al.* (1994) tested two different surface roughnesses and reported no differences in the friction coefficient for uncrowned pins when surface roughness was increased by a factor of three, but with

crowned pins an increase of about 30 percent was observed.

However, up to present it is not yet recognized in the open literature a deep and systematic study about the role of roughness under a technological point of view, in the tribological performance at high contact pressures and low sliding speed, such as parts of components for petroleum applications.

The aim of this paper is to evaluate the influence of surface roughness on the tribological performance of steel against steel under high pressure and low sliding speed conditions when a typical grease of the oil & gas industry is used. For this, the initial roughness level in Ra of the rings was systematically modified, varying between 1.3 and 3 microns. The relationship between the average roughness and maximum peak-valley roughness parameters with respect to the wear damage was analyzed. Also, the effect of varying the surface topography on the friction coefficient and its evolution were studied. These results were correlated with subsurface region affected by the tribological process.

II. METHODS

A. Tribotest, samples and test procedure

In order to reproduce the contact geometry and sliding conditions of the seal in OCTG connections, a lubricated block-on-ring test was used for the tribological evaluation. Figure 1 shows a sectional view of a typical threaded connection, highlighting the simulated sealing area and a schematic representation of the block-on-ring tribometer. This geometric configuration confined the lubricant between the contact surfaces because the block is in contact with the ring from the bottom.

The test parameters such as rotation speed, applied load and test time were chosen from the real contact conditions of the seal of a real tubular connection of 5.5 inches during the make & brake operations. This tube diameter has the worst contact conditions because it has the maximum sliding distance and must meet 10 cycles of make and break set by quality standards. Also, for simulating the make-up operation the load was increased linearly from a base load up to the maxim load. For the brake-out simulation load and rotation direction were alternated.

Block-on-ring tests were conducted under laboratory ambient conditions, at 25 ºC of temperature and 50 % of relative humidity. During each test, four complete cycles had been completed. Each cycle was composed of a charge stroke and a discharge stroke. The load in the charge stroke was varied linearly from 250 N to 7000 N and it was alternated at the discharge. The initial contact pressure was 230 MPa. Loading and unloading were carried out in opposite directions of rotation, providing a way for simulating the make-up and break-out of the actual oil & gas pipes connections.

The test samples design and their nominal dimensions are shown in Fig. 2. Rings were lathe machined with a diameter of 49.22 +0.025, −0.127 mm and a width of 7 ± 0.05 mm (Fig. 2 (a)). Blocks are prismatic square base of 12.32 ± 0.10 mm wide and 19.05 ± 0.41 mm long (Fig. 2 (b)) according to ASTM D 2509.

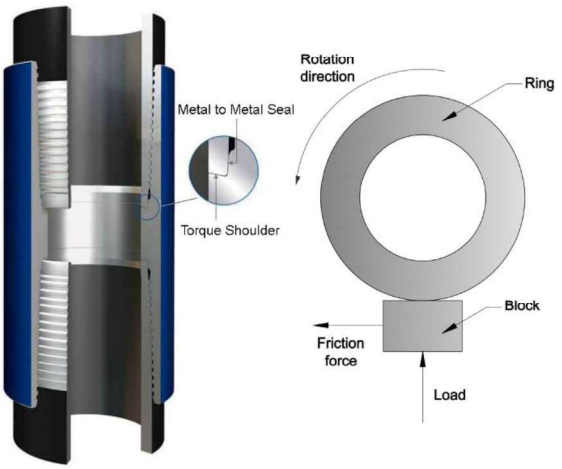

Fig. 1. Left: sectional view of a typical premium threaded connection, highlighting the sealing area; Right: schematic representation of the block-on-ring configuration used in wear tests.

Table 1. Chemical analysis of samples materials (wt%).

00	C	Mn	Ni	Si	Mo	Cr	P	S
Ring	.46	.69	.039	.306	--	.03	.015	.0072
Block	.44	.90	.031	.308	.17	.97	.018	.0019

Samples rings of AISI/SAE 1045 steel (233 HV_{10}) and blocks of AISI/SAE 4140 steel (270 HV_{10}) were made from as-received microstructural conditions. The chemical analysis of the samples materials was performed by optical emission spectrometry and is shown in Table 1.

Each stroke lasted 14 seconds, reaching a sliding distance of 409 mm. This was achieved after 2.65 revolutions of the ring rotating at 11 rpm, corresponding to a linear sliding speed of 30 mm/s. All the experiments were performed under ambient laboratory conditions (~25 °C, 65% relative humidity).

The friction force and load were measured using load cells and recorded as a function of time by a data acquisition system (Vernier Labquest). The coefficient of friction was calculated by dividing the friction force by the applied normal load.

As lubricant, a commercially available thread compound named Bestolife 72733, containing 65 % of lead, 1 % of copper, 5 % of zinc and 9% of graphite, has been used for all the tests conducted in this study. To ensure a homogeneous mixture, this lubricant was stirred before the beginning of each test. A method for applying lubricant was also developed, in which, at the beginning of each cycle, 0.1 g of dope (52.8 mm^3) was uniformly placed on the contact surface of the ring to simulate the actual make-up conditions of a real connection. The amount of lubricant was measured using a scale with 0.0001 g accuracy.

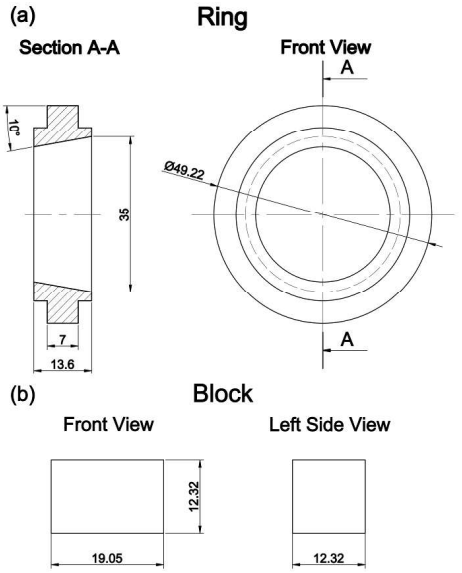

Fig. 2. Samples design and geometry.

Upon completion of the test, worn surfaces were examined by optical and laser scanning microscopy. Wear was assessed by measuring the volume of the material removed from the block using optical microscopy (OM) and a specific software according to ASTM G 77 standard. The worn volume was calculated using five width measurements across the worn track. This procedure was repeated three times for each test in order to minimize errors due to focus and measuring.

Additionally the final roughness and profile of the contact surface of the ring was measured. Moreover, the block worn surfaces were cross-sectioned and analyzed with OM, scanning electron microscope (SEM) and micro-vickers hardness indentations; then, the dominated wear mechanisms were discussed in detail.

B. Roughness characterization

As mentioned above, from the technological point of view the most used surface roughness parameter is R_a. Tests were performed by changing the surface roughness of the rings between R_a values from 1.3 to 3 μm. The surface condition was achieved by lathe machining the rings and controlled with a roughness profilometer contact stylus (Hommel Tester T500) using a 4.8 mm cut-off length.

In order to obtain accurate results, each contact surface of the ring was measured 10 times.

After the rings were machined, some of them had similar or identical R_a value, but their contact surface profile were different. These differences could be seen from the comparison of other roughness parameters. Due to this, besides the R_a parameter, the trend of the roughness parameter R_t was also taken into account. The value of R_t indicates the vertical distance between the lowest and highest points of the filtered roughness profile within the reference length.

III. RESULTS AND DISCUSSION

A. Wear behavior of the ring sample

The surface profiles of the rings before and after the tests are shown in Fig. 3, where the typical profile with an initial R_a and R_t values of 2.85 μm and 18.88 μm, respectively is shown. After the tribotest, a reduction of 3.32 μm in the R_t value was observed (Fig. 3 (b)). The wear of the rings was localized on the peaks, forming plastically deformed ridges. This condition was inferred by comparing the profiles in Fig. 3.

B. Wear mechanisms observed on ring samples

It is well established that when any rough surface is in contact with a hard surface, the actual contact area is only a small proportion of the apparent contact surface (Pearsson, 2001). As in the assembly process of actual oil connections, surface ridges were worn during tests, thus altering the topography of the surface.

Since the contact pressure is very high in the tubular connections, it is expected an important surface wear and plastic deformation of the asperities. Therefore, it is unrealistic to expect the elastic deformation of the surface asperities.

The plasticity index ψ is an indicator of the level of deformation (elastic or plastic) reached in surface ridges. It is a dimensionless value that depends on the surface topography and mechanical properties of the materials in contact. Greenwood and Williamson were the first who define it as shown in Eq. (1).

$$\psi = \frac{E^*}{H}\left(\frac{\sigma^*}{R}\right)^{1/2} \quad (1)$$

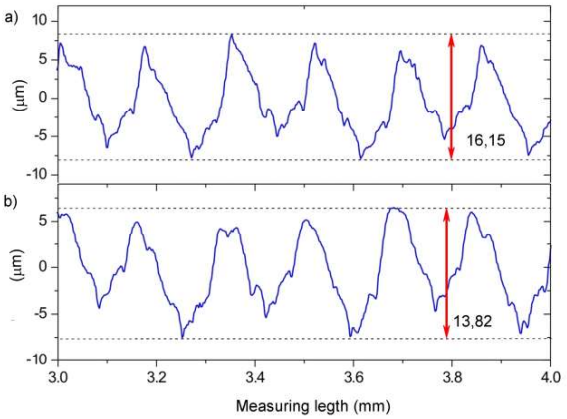

Fig. 3. Surface profiles of a ring with initial R_a = 2.85 μm: (a) before testing; (b) after testing.

where $E^* = E/(1-\nu)$, being E the Young's modulus and ν the Poisson's ratio, H the hardness, σ^* the standard deviation of asperity height distribution and R the average radius of the rough ridges.

When $\psi < 1$, ridges are elastically deformed, whereas when $\psi \geq 1$ indicates that even under very small contact pressures, most of the surface asperities are plastically deformed.

Then, from the approximation of Greenwood and Williamson, several authors proposed different approaches to determine ψ based on other surface parameters. Mikić (1974) proposed an alternative definition of the plasticity index parameter based on the root mean square slope of the surface profile σ_m, which is shown in Eq. (2):

$$\psi = \frac{E^*}{H}\sigma_m \quad (2)$$

This definition avoids the difficulty of determining the two statistical quantities involved in other definitions of ψ and that are not independent.

Applying the proposed Mikic model the values of ψ were determined for the different initial ring surfaces of this study. As expected, these were greater than one, varying in the range from 5.7 to 8.8, corresponding to the rings profiles with lower and higher roughness, respectively.

Once the surface ridges were plastically flattened, subsequent plastic deformation of the asperities was produced by sliding wear. Therefore, based on the analysis of the evolution of the surface topography (see Fig. 3), it follows that the damage on the rings was promoted by the mutual interaction of two micro-mechanisms. The local plastic deformation of surface ridges (flattening) and the burnishing of those rough asperities. These observations are consistent with the work of Le *et al.* (2015) by observing the burnished surface asperities due to plastic deformation and wear.

C. Wear performance of block samples

The worn volume results as a function of the initial R_a ring roughness are shown in Fig. 4. Each dot corresponds to one test with error bars indicating the scatter in the roughness and wear measurements. A wear reduction of about 40 percent with increasing ring roughness was noticed. A possible explanation to this observed tendency is that the rougher surfaces retained a bigger amount of lubricant thus reducing wear damage. The lubricant would be then lodged between the grooves left by the cutting tool during turning.

The large scatter of the wear results after R_a= 2.0 µm could be explained by the incidence of the roughness parameter R_t. In this sense, the arrow displayed in Fig. 4 denotes the wear reduction tendency with the value of R_t. It is known that for surfaces with similar R_a values, when the R_t value is higher, the distance between the highest peak and the lowest valley is increased. These could provide even more lubricant retention.

In addition, the influence of the R_t parameter in the wear behavior is graphed in Fig. 5, where the ratio of wear volume to R_t was plotted as a function of the initial R_a value. It was demonstrated that the relation between those parameters was well correlated by an exponential function. A regression study of these results was performed using statistical software (Di Rienzo *et al.*, 2008), resulting in the exponential model shown in Eq. (3). This analysis indicated that the estimation of the model parameters was highly significant. Moreover, the studentized residuals showed that the regression model assumptions were verified and that the unobservable errors were well controlled by the proposed exponential model. Moreover, for better understanding of the effect of the R_t parameter, a graph showing the interaction between R_a and R_t is presented in the inset graph of Fig. 5.

$$\text{Wear Vol} / R_t = 0.07 \cdot \exp(-0.62 \cdot R_a) \quad (3)$$

$$\text{Wear Vol} = 0.07 \cdot R_t \cdot \exp(-0.62 \cdot R_a) \quad (4)$$

From the relationship modeled by Eq. (3), it is possible to obtain Eq. (4), which shows the relationship of the worn volume in terms of the roughness parameters R_a and R_t.

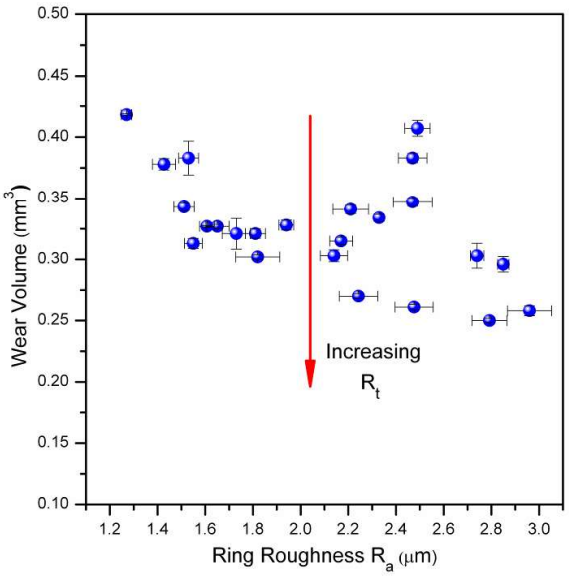

Fig. 4. Worn volume graph as a function of the initial roughness.

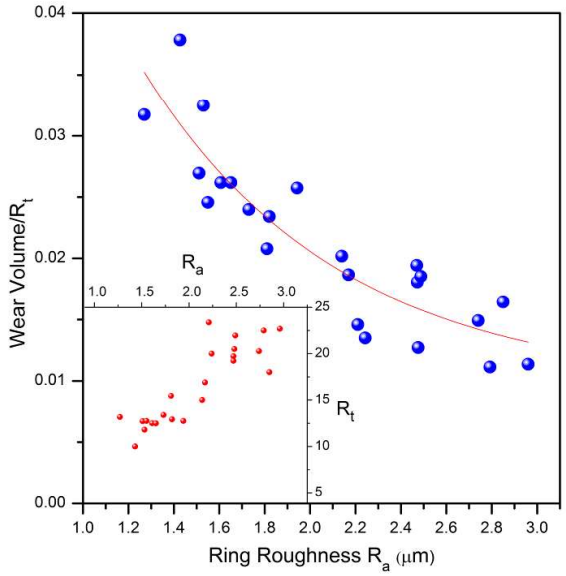

Fig. 5. The ratio of wear volume to R_t as a function of the initial value of R_a. Inset graph: Relation between R_a vs R_t.

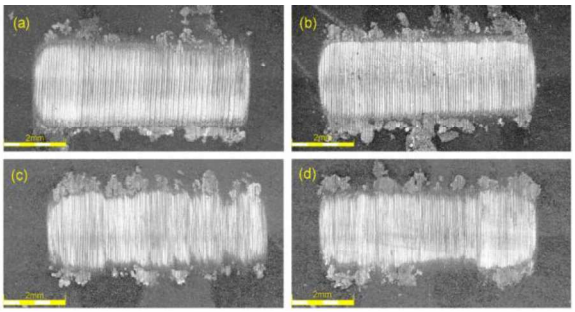

Fig. 6. LSCM images comparing the wear scars of four characteristic tests: (a) R_a= 1.43 μm; (b) R_a= 2.14 μm; (c) R_a= 2.24 μm; (d) R_a= 2.79 μm.

Knowing the values of R_a and R_t the proposed Eq. (4) allows to estimate the wear.

D. Wear mechanism observed in blocks samples

Figure 6 shows laser scanning confocal microscopy (LSCM) images of the wear scars of four characteristic tests. Figure 6 (a) and Fig. 6 (d) correspond to the tests with the lowest and highest initial roughness, respectively. Figure 6 (b) and Fig. 6 (c) showed a transition in the severity of damage, mainly on the edges of the wear track. This transition occurs when the initial R_a roughness value of the ring exceeded 2.2 μm.

As can be seen from Fig. 7 and Fig. 8, the metallographic analysis of the surface layer beneath a wear track revealed near-surface cracks lying parallel to the surface, slivers at an acute angle and a plastically deformed region (PDR) on the sub-surface. The severe plastic strains developed in the PDR suggested that wear was driven by plastic strain. Moreover, Fig. 7 reveals signs of turbulent plastic flow produced normally to the sliding direction. These plastic flow-lines were observed in both tests with extreme roughness, nevertheless they were more intense in the smoother (Fig. 7 (a)), also confirming its high wear.

Therefore, these results show that the wear behavior was dominated by accumulated plastic shear flow (low-cycle ratchetting) under microploughing conditions that led to subsuperficial crack initiation and propagation (delamination wear).

The plastic deformation developed during friction process was a result of the low-cycle ratchetting produced under microploughing conditions. These large permanent strains were acquired through the accumulation of small increments occurring with each cycle of repeated load due to many abrasive particles. As postulated Zum Gahr (1987) and Johnson (1995) a prow can be formed ahead of the abrading particles and material is continually displaced sideways to form slivers adjacent to the groove produced. This seems to be in agreement with the slivers showed in Fig. 7 (a) and Fig. 9. The low-cycle ratchetting by microploughing promotes wear by extrusion into thin slivers, so fracture does not control the wear rate (Johnson, 1995; Kapoor 1994; Kapoor 1997).

Apart from that, during sliding, the sub-surface material that does not extrude out, keeps on accumulating plastic deformation and may break off by low cycle fatigue (delamination wear). Figure 9 shows, after a few friction cycles, sub-surface cracks confirming the presence of delamination wear. This is in accordance with the work reported by Jahanmir and Suh (1977) who studied the mechanics of sub-surface void nucleation in delamination wear and concluded that voids can nucleate after 1 - 10 asperity passes and that the number of passes required for void nucleation decrease with increasing COF. Then, the surface fails by either low cycle fatigue or ratchetting failure and delaminates.

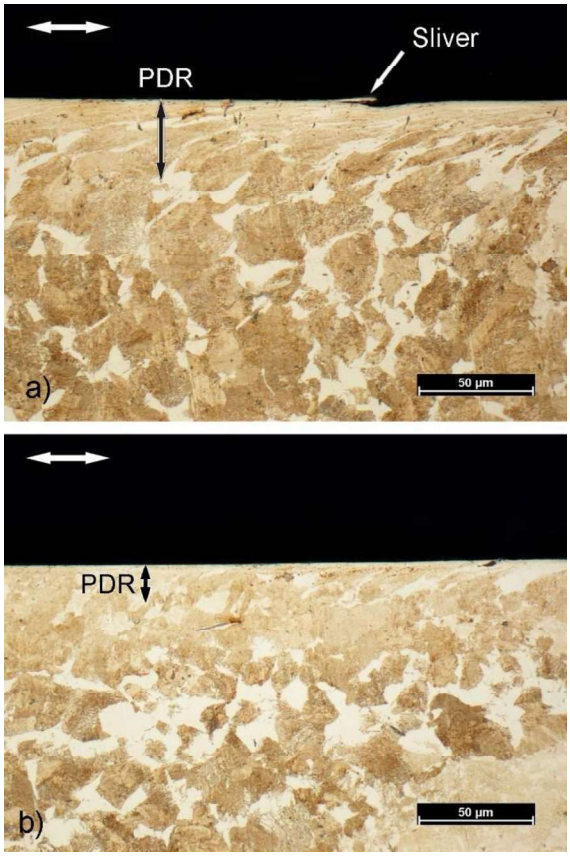

Fig. 7. Optical microscopy (OM) micrographs in side view of the wear scar in block specimens sectioned in the sliding direction. (a) test with R_a= 1.27 μm. (b) test with R_a= 2.96 μm.

On the other hand the plastic flow lines of the PDR aligned with the sliding direction and in the sense during load strokes shown in Figs. 7 and 8 were also observed by others researchers under bidirectional reciprocating sliding (Long and Rack, 2005). This plastic flow was mainly promoted during the first charge stroke, where the higher stress by non-conforming contact conditions took place. Besides, this condition is in coincidence with the COF difference between loads and unloads strokes, where the COF value was higher at the load ones.

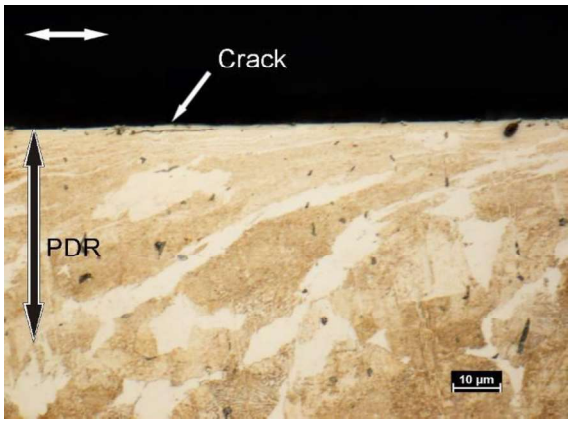

Fig. 8. OM micrograph in side view of a block tested with R_a= 1.27 µm (sectioned in the sliding direction).

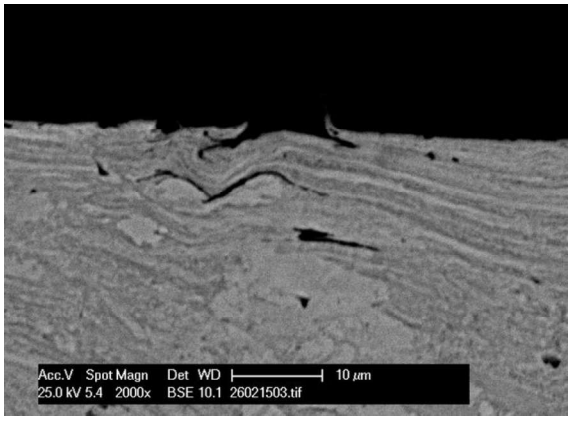

Fig. 9. Scanning electron microscope (SEM) micrograph in side view of the wear scar in a section normal to the sliding direction of a block specimen tested with R_a= 1.27 µm.

Moreover, Kapoor (1997) hypothesized that if the sliding direction is reversed at each cycle, then the cycle of plastic strain is closed (no net accumulation of strain); he experimentally observed in some tests that despite the fully reversed nature of the axial load, some specimens ratchetted. This effect was also observed before by Benham and Ford (1961) when tested mild steel specimens subjected to fully reversed load cycles and found that some specimens accumulated a plastic extension in each cycle.

As it was mentioned before, in the fixed samples with low roughness, which had higher wear volumen, an extensive PDR was promoted by a high ratchetting level (see Figs. 7a and 8), due to the poor lubricant retention capability of the smoothest surfaces, which produced an increase in the shear stress between the contact surfaces. The higher level of wear is a consecuence of extensive deformation that led to the formation of subsurface cracks, which eventually grew by delamination wear (see Fig 7 a).

While, the PDR was observed in all the fixed samples, the plastic deformation produced by the rings with higher roughness was small, since the higher roughness increase the lubrication availability in the contact zone, contributing to protect the surface and minimizing to the wear damage.

E. Friction behavior

On the whole, the friction coefficient values from the block-on-ring tests showed similar patterns. In Fig. 10 a typical set of results for a charge stroke of a block-on-ring test is presented. As can be seen from the graph, the normal load, friction force and coefficient of friction are all plotted as a function of the time. Furthermore, the values of the coefficient of friction are in line with those published by Stewart *et al.* (2012) using a cross-cylinder friction test rig setup for the range of contact pressure evaluated in the current research.

Also, a marked decrease in the COF value with the completion of the ring revolutions after 5.2 sec and 10.4 sec was observed (Fig. 10). This is in good agreement with the running-in stage where the friction decreases when the surface asperities become burnished.

Since the surface roughness changes dramatically, especially at the beginning of the test, the influence of surface roughness on friction was evaluated by plotting the average COF in the first two seconds of the test as a function of the initial ring roughness (Fig. 11). An increase in the COF value with the decreasing roughness was observed.

As mentioned above, this higher friction caused in the tests with less roughness produced more plastic deformation, thus increasing the wear damage. These results suggest that the COF increase may be due to the growth of the real contact area on account of the decreasing roughness, i.e. with smooth surfaces the friction tends to be high because the real area of contact grows (Rabinowicz, 1995). Moreover, this higher friction could be explained by the inability of the smoother surfaces to retain lubricant, leading the surfaces exposed to direct metal-metal contact (Furey *et al*, 1963; Jeng *et al*, 1990)

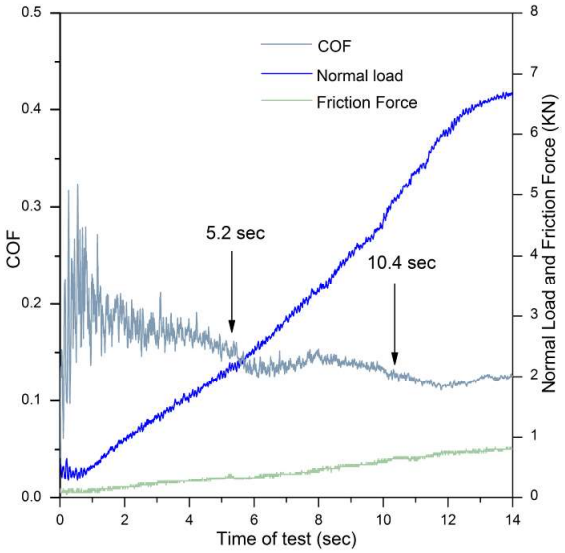

Fig. 10. Graphic of behavior of normal load, friction force and friction coefficient with time during a charge stroke.

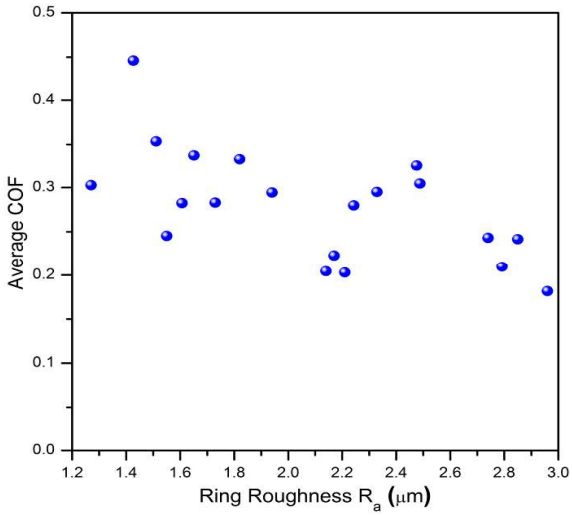

Fig. 11. Average COF of the first 2 seconds of the test as a function of the initial roughness.

As illustrated by Fig. 12, the evolution with time of the friction behavior in the first charge stroke for the tests with the highest and lowest roughness is presented. It was observed that increasing the surface roughness from 1.43 μm to 2.96 μm of R_a, reduces the COF value for about 40 percent.

A similar tendency was reported by other authors who pointed out that under dry conditions, the dominant wear mechanism was abrasion and the COF was lower when roughness was higher (Sedlaček *et al*, 2009). Also the same behavior was reported by Khun *et al.* (2014).

Furthermore, Carper *et al.* (1994) with the same kind of test reported an increment in the COF value of about 30 percent by using crowned pins when the roughness R_a value change from 0.5 μm to 1.5 μm. The discrepancies from the work of Carper et al. with the results presented in this paper could be explained by the different geometric design of the tests and the possible incidence of the hydrodynamic lubrication in Carper's tests.

Also a difference in the COF behavior between loads and unload was observed during each cycle, where COF was steady and slightly lower in the unload strokes. This COF difference may contribute in the directionality of plastic flow mentioned above. This behavior is in accordance with Johnson (1995) and Kapoor (1994) who concluded that with greater friction increases the sub-surface deformation and the plastic strains per cycle leading to a higher wear rate.

IV. CONCLUSIONS

From the evaluation of the influence of surface roughness in the steel / steel tribosystem lubricated with thread compound and evaluated at low speed and high load, the following conclusions may be drawn:

- When the roughness was increased in the moving surface, an improvement of ~40% in the wear resistance was found for the fixed component. We propose an exponential negative correlation between the initial R_a and R_t roughness parameters of the moving counterpart and the wear volume of the fixed material can be inferred from the wear results.
- Under lubricated sliding on high pressure contact conditions, the protuberances of the moving surface were plastically deformed and burnished due to the tribological process.
- In the fixed component, the sinergy between low cycle ratchetting mechanism and delamination wear were the responsible for the damage.
- For the oil and gas industry, although the friction results evidenced an increase in the COF value when ring roughness decreased, it is recommended a high roughness to reduce wear. The results of this research can be used to improve the design conditions of OCTG connections.

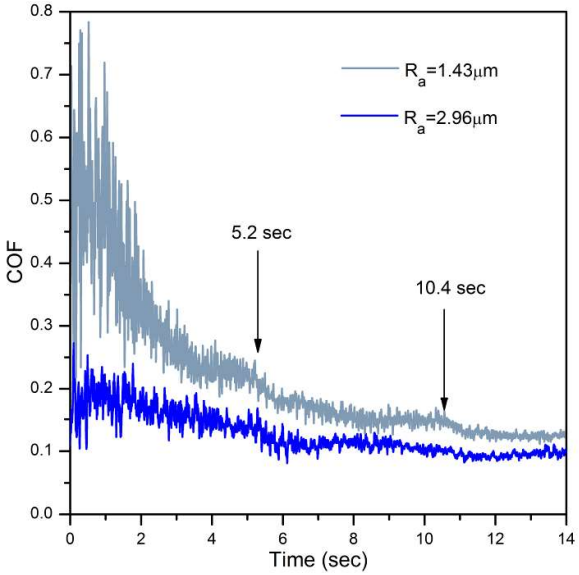

Fig. 12. Variation of COF with the time in the initial charge stroke for the tests with the highest and lowest roughness.

ACKNOWLEDGEMENTS

The authors would like to acknowledge the support given by the Engineering Department of Universidad Nacional del Sur, CONICET and especially Patricia Santos Biasotto from OLYMPUS.

REFERENCES

Benham, P.P. and H. Ford, "Low endurance fatigue of a mild steel and an aluminium alloy," *J. Mech. Eng. Sci.*, **3,** 119-132 (1961)

Bollfrass, C.A., "Premium connections require proper planning and selection," *Petrol. Eng. Int.*, **55**, 28-43 (1983).

Carper, H.J., A. Ertas, J. Issa and O. Cuvalci, "Effect of some material, manufacturing, and operating variables on the friction coefficient in OCTG connections," *J. Tribol.*, **114**, 698-705 (1992).

Carper, H.J., A. Ertas and O. Cuvalci, "Effect of contact geometry and other tribological variables on

the friction coefficient in threaded connections," *ASME J. of Mech. Design,* **61**, 117-122 (1994).

Carper, H.J., A. Ertas and O. Cuvalci, "Rating thread compounds for galling resistance" *J. Tribol.*, **117,** 639-645 (1995).

Di Rienzo, J.A., F. Casanoves, M.G. Balzarini, L. Gonzalez, M. Tablada and C.W. Robledo, *InfoStat*, version 2008, Grupo InfoStat, FCA, UNC, Argentina (2008).

Ertas, A., O. Cuvalci and H.J. Carper Jr., "Determination of friction characteristics of J-55 OCTG connections lubricated with environmentally safe thread compound," *Tribol. T.*, **42** 881-887 (1999).

Furey M.J., "Surface Roughness Effects on Metallic Contact and Friction," *ASLE Trans.,* **6**, 49-59 (1963).

Jahanmir, S. and N.P. Suh, "Mechanics of subsurface void nucleation in delaminat ion wear," *Wear*, **44**, 17-38 (1977)

Jeng, Y.R., "Experimental Study of the Effects of Surface Roughness on Friction," *Tribol. T.*, **33**, 402-410 (1990).

Johnson, K.L., "Contact mechanics and the wear of metals," *Wear,* **190**, 162-170 (1995).

Kapoor, A., "A re-valuation of the life to rupture of ductile metals by cyclic plastic strain," *Fatigue Fract. Eng. M.,* **17**, 201-219 (1994).

Kapoor, A., "Wear by plastic ratchetting," *Wear*, **212**, 119-130 (1997).

Khun, N.W., G.S. Frankel and M. Sumption, "Effects of Normal Load, Sliding Speed, and Surface Roughness on Tribological Properties of Niobium under Dry and Wet Conditions," *Tribol. T.*, **57,** 944-954 (2014).

Le, H.R., F. Stewart and J.A. Williams, "A Simplified Model of Surface Burnishing and Friction in Repeated Make-Up Process of Premium Tubular Connections," *Tribol. Lett.*, **59,** 1-11 (2015).

Long, M. and H.J. Rack, "Subsurface deformation and microcrack formation in Ti–35Nb–8Zr–5Ta–O (x) during reciprocating sliding wear," *Mater. Sci. Eng. C*, **25**, 382-388 (2005).

Matsuki, N., Y. Morita and H. Kawashima, "Evaluation of premium connection design conditions," *ASME, Energy Resources Technology Conference and Exhibition*, **PET-8** (1985).

Mikić, B.B., "Thermal contact conductance; theoretical considerations," *Int. J. Heat Mass Tran.*, **17**, 205-214 (1974).

Muster, A. and W. Presz, "Influence of Initial Surface Roughness on Galling Behaviour of a Steel- Steel Couple," *Scand. J. Metall.* **28**, 5-8 (1999).

Pearsson, B.N.J. "Elastoplastic contact between randomly rough surfaces," *Phys. Rev. Lett.*, **87,** 116101, 1-4 (2001).

Rabinowicz, E., *Friction and wear of materials*, 2nd Edition, John Wiley & Sons, Inc., New York, United States (1995).

Sedlaček, M., B. Podgornik and J. Vižintin, "Influence of surface preparation on roughness parameters, friction and wear," *Wear*, **266**, 482-487 (2009).

Stewart, F., H.R. Le, J.A. Williams, A. Leech, B. Bezensek and A. Roberts, "Characterisation of friction and lubrication regimes in premium tubular connections," *Tribol. Int.*, **53,** 159-166 (2012).

Zum Gahr, K.H., *Microstructure and wear of materials*, Elsevier Science Publishing Company Inc., New York, USA, **10** (1987).

Received: March 30, 2017.
Sent to Subject Editor: April 19, 2017.
Accepted: May 6, 2019.
Recommended by Subject Editor: Eduardo Dvorkin and Chief Editor: Alberto Bandoni